Supplementary Materials for

DNA-guided lattice remodeling of carbon nanotubes

Zhiwei Lin[1*], Leti Beltran[2], Zeus A. De los Santos[1], Yinong Li[3], Tehseen Adel[4], Jeffrey A Fagan[1], Angela R. Hight Walker[4], Edward H. Egelman[2], and Ming Zheng[1*]

[1]Materials Science and Engineering Division, National Institute of Standards and Technology, Gaithersburg, MD 20899, USA
[2]Department of Biochemistry and Molecular Genetics, University of Virginia, Charlottesville, VA 22908, USA
[3]South China Advanced Institute for Soft Matter Science and Technology, School of Emergent Soft Matter, South China University of Technology, Guangzhou 510640, China
[4]Quantum Metrology Division, National Institute of Standards and Technology, Gaithersburg, MD 20899, USA

* zhiweilin@scut.edu.cn; ming.zheng@nist.gov

Disclaimer: *Certain equipment, instruments or materials are identified in this paper in order to adequately specify the experimental details. Such identification does not imply recommendation by the National Institute of Standards and Technology (NIST), nor does it imply the materials are necessarily the best available for the purpose.*

This PDF file includes:

Materials

CoMoCAT SWCNT powders (SG65i grade, lot no. L64) were obtained from Southwest Nanotechnologies. Oligomers of ssDNA were purchased from Integrated DNA Technologies. Polyethylene glycol (PEG, MW 1.5 kDa, Alfa Aesar), polyethylene glycol (PEG, MW 6 kDa, Alfa Aesar), dextran (DX, MW 250kDa, Alfa Aesar), polyvinylpyrrolidone (PVP, MW 10 kDa, Sigma-Aldrich), sodium phosphate dibasic (Na_2HPO_4, Sigma-Aldrich), sodium phosphate monobasic (NaH_2PO_4, Sigma-Aldrich), phosphoric acid (H_3PO_4, 85%, MCB Reagents), sodium thiocyanate (NaSCN, Sigma-Aldrich), sodium chloride (NaCl, BDH Chemicals), rose bengal (RB, dye content 95%, Sigma-Aldrich), phosphate buffer solution (NaPB, 1M, pH=7.4, Sigma-Aldrich), sodium deoxycholate (DOC, Sigma-Aldrich) were used as received.

UV-Vis-NIR absorption spectroscopy

UV-Vis-NIR absorption spectra were collected on a Cary 5000 spectrophotometer using a 1 cm path length quartz microcuvette. The volume for each analysis was typically 0.1 mL and all spectra were obtained with background subtraction.

PL and Raman spectroscopy

Photoluminescence (PL) and Raman spectra were collected using an NS3 Nanospectralyzer (Applied NanoFluorescence, Houston, TX) with two excitation wavelengths (532 and 671nm). The sample volume was typically 0.4 mL and all spectra were obtained at room temperature. Spectra were collected in presence of 0.25% DOC. The Raman $I_{D/IFM}/I_G$ ratio was calculated using peak intensities. We have also tried peak fitting followed by peak area integration to obtain intensities of defect- and G-peak and their ratio. These two methods yield similar results.

Purification of SWCNTs

DNA-SWCNT dispersions were prepared according to procedures reported previously (*27*, *28*). Typically, SG65i-L64 SWCNT powders (1 mg) and ssDNA sequence (2.5 mg) are sonicated in either sodium phosphate buffer (30 mmol/L at pH = 4) for purification of GC_4G-(+)(6,5) and $(GCGCCC)_6$-(9,1), or sodium chloride (30 mmol/L) in aqueous solution for purification of $TTA(TAT)_2ATT$-(–)(6,5) and $T_3C_3T_3C_6$-(–)(8,3), giving 1 mg/mL of SWCNT-DNA dispersion.

$TTA(TAT)_2ATT$-(–)(6,5) and $T_3C_3T_3C_6$-(–)(8,3) were purified according to procedures reported previously (*29*). For the purification of GC_4G-(+)(6,5) and $(GCGCCC)_6$-(9,1), the following procedures were proceeded. Separate solutions of PEG 1.5 kDa and DX 250 kDa aqueous two-phase (ATP) stock solution (with two compositions 10:0 and 7:3) were prepared following the procedures identified in our previous publication (*30*). The mass fraction (%) of PEG 1.5kDa and DX 250kDa are 8.57 and 10.1 in 10:0 stock solution, and 12.2 and 14.4 in 7:3 stock solution, respectively. In a typical partition experiment, 3 volumes (120 μL) of SWCNT-DNA dispersion was loaded into 7 volumes (280 μL) of the 7:3 stock solution, giving a 10:0 ATP system at room temperature. In the first step, 2 μL 1% PVP (10 kDa) in water was added into the 10:0 ATP system. The mixture was vortexed and subsequently centrifuged and the first top fraction (1T) was extracted. 1T fraction containing either (+)(6,5) or (9,1) species was further incubated at 4 °C overnight, inducing a new two-phase separation. The new top fraction (1T-T) with a higher purity of (+)(6,5) or (9,1) species was collected and the SWCNT-DNA hybrids were precipitated by adding NaSCN to a final concentration of 0.5 mol/L. The supernatant liquid was completely removed. The pellets were resuspended in 20 mmol/L NaPB buffer (pH=7.4) to give pure SWCNT species with a concentration of OD ~20.

One-pot Chemistry

One-pot reaction to produce various functionalized DNA-SWCNTs were performed following a similar procedure. Here, we use 2G-7 ($C_3GC_7GC_3$)-functionalized (8,3) as an example to demonstrate a typical reaction. Into 10 μL $T_3C_3T_3C_6$-(8,3) with OD ~20, 6 μL NaPB buffer (20 mmol/L, pH=7.4), 2 μL 10% DOC and 6 μL 2G-7 (10 mg/mL) were added and vortexed. 105 μL MeOH was dropwise (5 μL/drop) added into the mixture under a vigorous vortexing condition. In this step, $T_3C_3T_3C_6$ are removed from (8,3) nanotubes, and 2G-7 are wrapped onto nanotubes, which is a process of DNA-DNA exchange. Then, 80 μL NaPB buffer (20 mmol/L, pH = 7.4) and 1 μL RB (6 mmol/L) was added into the mixture to reach a 50% v/v MeOH content. The entire reaction mixture contained in a 5 mL glass vial was stirred and illuminated by a pair of 525 nm LED lamps (PR160 Rig with Fan kit, Kessil) for 1 hour at room temperature. Note that the DNA-DNA exchange and the reaction take place in one-pot. With 50 times excess reacting DNA, replacement of the original wrapping DNA is estimated to be more than 98% complete. Any residue original wrapping DNA should be further replaced by the reactive G-containing sequences during the functionalization reaction. After reaction, the functionalized nanotubes were precipitated by adding NaSCN (5 mol/L) to a final concentration of 0.5 mol/L, and centrifuged at 17,000 G (G = 9.81 m/s^2) for 10 minutes. The supernatant liquid was completely removed. The pellets were resuspended in 20 mmol/L NaPB buffer (pH = 7.4) for further characterization. The unfunctionalized 2G-7 control sample used for cryo-EM characterization was prepared by following the above procedure without adding RB and going through the illumination.

Cryo-EM Sample Preparation and Data Collection

Sample containing either covalently linked 2G-5-, 2G-6-, 2G-7-(8,3) or unfunctionalized 2G-7-(8,3) carbon nanotubes at a concentration of OD ~5-10 was diluted 1:10 in distilled water, which has been passed through an ion exchange filtration system. In brief, a 2μL aliquot of sample was applied to a plasma-cleaned (Gatan Solarus) lacey carbon grids (Ted Pella, INC.), blotted with automated blotting for 3 s at 90% humidity and flash frozen in liquid ethane using an EM GP Plunge Freezer (Leica). The dataset used for structure determination was collected at the Molecular Electron Microscopy Core at the University of Virginia on a Titan Krios EM operated at 300 keV, equipped with an energy filter and K3 direct electron detector (Gatan). An energy filter slit width of 10 eV was used during data collection and was aligned automatically every hour. All 18,404 covalently linked 2G-7-(8,3) and 17,471 unfunctionalized 2G-7-(8,3) movies were collected in counting mode at a magnification of 105 K, pixel size of 0.86 Å. Data collection was performed using a total dose of 80 e^- $Å^{-2}$ across 60 frames at a rate of 4.80 s/movie.

Data Processing

Unless otherwise stated, all data processing was completed using cryoSPARC v3.2.0. Movies were corrected for full-frame motion using Patch Motion Correction followed by Gctf CTF Estimation. After CTF estimation, micrographs were sorted and selected based on estimated resolution (0 to 4Å), defocus (0.6 to -2.6 μm), ice thickness, and total full-frame motion. Initial particles were automatically picked using 'Filament Tracer' with a filament diameter of 100 Å and a separation distance of 0.1. Particles were extracted at a box size of 256 pixels, followed by

2D classification. Class averages containing filaments distinguishable from that of noise were selected for template-based particle picking. A total of 29,453,362 particles were extracted using a box diameter of 260 Å. These particles were sorted using 2 iterative rounds of 2D classification with 50 classes each, number of online-EM iterations set to 20 and a batch size of 100 per class. The final iteration of 2D classification yielded a subset of 44,393 particles. Reconstructions of the 2G-7-(8,3) carbon nanotube was generated by two methods (1) an averaged power spectrum was generated using the raw images of aligned filament segments selected from 2D classification. A single layer line observed with a spacing of 6.5 Å from the meridian was used for helical averaging to produce a 3D map with all details smeared out, (2) an initial model was generated using an unbiased approach '*Ab-initio* reconstruction', class size set to 1. An output 3D map was inspected for structural motifs (i.e., ssDNA chain around a tube). Particles were further refined using iterations of homogeneous refinement with the input volume generated by single-class *ab initio*. A 3D map possessing low-resolution features was sharpened using a negative B-factor of 19.1.

The unfunctionalized 2G-7-(8,3) carbon nanotube movies were subjected to the same automated particle picking, sorting, and selecting protocol as the functionalized sample. A total of 11,873,739 particles were extracted using a box diameter of 256 Å and these particles were sorted using one round of 2D classification with 50 classes. Raw images of aligned filament segments, selected from 2D classification were used to generate an averaged power spectrum.

MD simulation

The GROMACS 2018.6 simulation package was used in conjunction with the CHARMM27 force field for MD simulation. The structure of (8,3) was created in VMD and the structure of $C_3GC_7GC_3$ (2G-7) was created in GROMACS. For the initial structure, three DNA strands of 2G-7 with the direction of 5'-3', 3'-5' and 5'-3' were sequentially placed around the (8,3), and the C_8 atom of guanine was covalently conjugated with a C-C bond on an armchair line. The functionalized 2G-7-(8,3) was solvated in a 50.0×50.0×83.7 Å water box. It contains around 6000 TIP3P model water molecules with the appropriate amount of sodium counterions to balance the negative phosphate charges. The final structure was obtained by energy minimization and annealing with a maximum temperature of 500 K. The final frame was visualized in VMD.

Table S1. DNA sequences of different G contents used in Fig. 2.

Sequence	G content (%)
GC_{11}	8.3
$GC_{13}G$	13.3
$(CCGCCC)_3$	16.7
$(GCCCCG)_3$	33.3
$(GCGCGC)_3$	50.0
$(GCCGGG)_3$	66.7

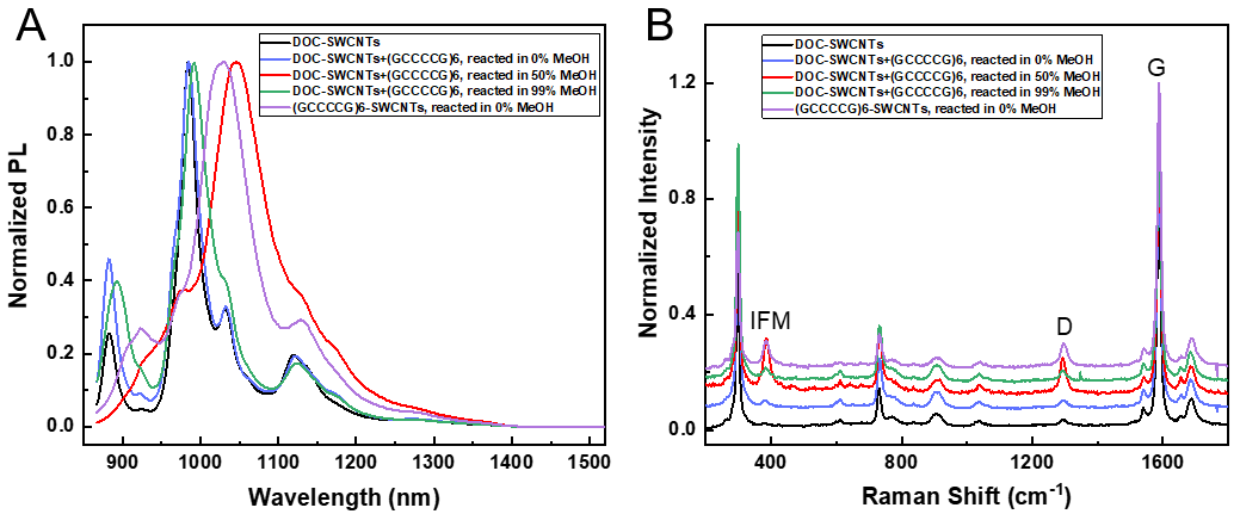

Fig. S1. (A) PL spectra and (B) Raman spectra of $(GCCCCG)_6$-functionalized SG65i SWCNTs under various conditions. **Black trace:** DOC-coated non-functionalized SWCNTs (serving as a control); **blue trace:** DOC-coated SWCNTs + $(GCCCCG)_6$, reacted in 0% MeOH; **red trace:** DOC-coated SWCNTs + $(GCCCCG)_6$, reacted in 50% MeOH; **green trace:** DOC-coated SWCNTs + $(GCCCCG)_6$, reacted in 99% MeOH; **purple trace:** $(GCCCCG)_6$-wrapped SWCNTs reacted in 0% MeOH.

Discussion on Fig. S1: To optimize the functionalization condition, we carried out the reaction between $(GCCCCG)_6$ and SG65i SWCNTs at 0%, 50% and 99% MeOH content, respectively. It is evident that no reaction occurs at 0% MeOH (blue trace), as DOC can't be replaced by G-containing DNA under this condition. On the other hand, at 99% MeOH the reaction is dramatically hindered due most likely to slowed singlet oxygen production (green trace). In contrast, 50% MeOH appears to be an optimal condition to enable both DOC/DNA exchange and singlet oxygen production. We also show in this experiment that reaction with DOC/DNA exchange at 50% MeOH results in more complete functionalization than that achieved with DNA-SWCNTs, which was prepared by direct sonication, as the starting material in aqueous solution (red trace *vs* purple trace in the figure).

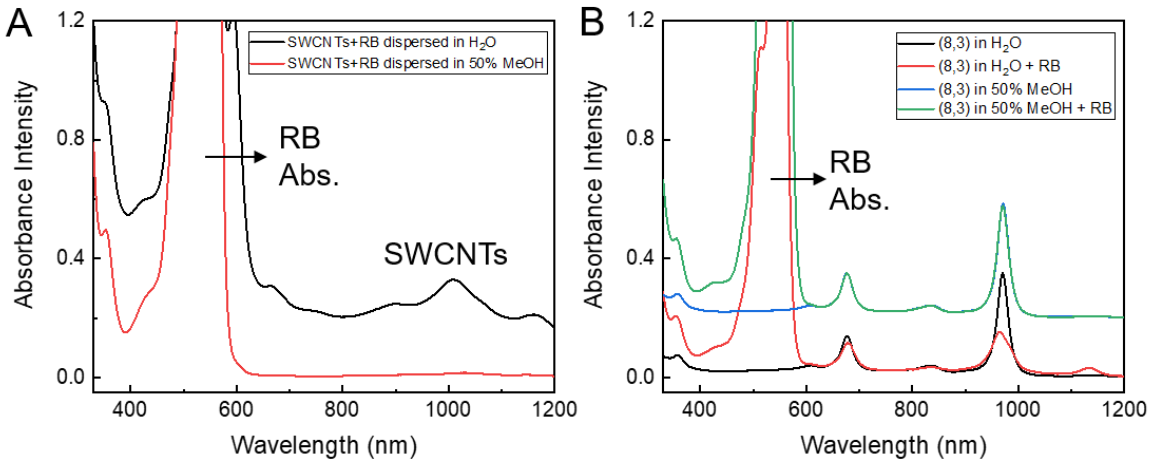

Fig. S2. (A) Absorbance spectra of rose Bengal (RB) dispersed SG65i-SWCNTs in water and 50% MeOH. (B) Absorbance spectra of GGCCGG-(8,3) in water and 50% MeOH, and in the absence and presence of 30 μM RB.

Discussion on Fig. S2: As an aromatic dye molecule, rose Bengal (RB) is expected to have binding affinity with SWCNTs via π-π stacking interaction. To clarify if RB interferes with DNA wrapping during the reaction (in 50% MeOH), a set of experiments were designed. (i) 1% (w/w) RB was used to disperse SWCNTs in water and 50% MeOH by sonication, respectively. As shown in **Fig. S2A**, 1% (w/w) RB can disperse SWCNTs in water, but not in 50% MeOH. This suggests that RB has much weaker binding affinity with SWCNTs in 50% MeOH than in water. (ii) Absorbance spectra of GGCCGG-(8,3) was measured in water and 50% MeOH with and without RB. As shown in **Fig. S2B**, addition of 30 μM RB to GGCCGG-(8,3) causes decreased E_{11} peak in water (black trace vs. red trace) but not in 50% MeOH (blue trace vs. green trace). It indicates that RB does not interfere with DNA in 50% MeOH. We thus conclude that MeOH minimize RB binding to SWCNTs and RB does not affect DNA conformation during the reaction.

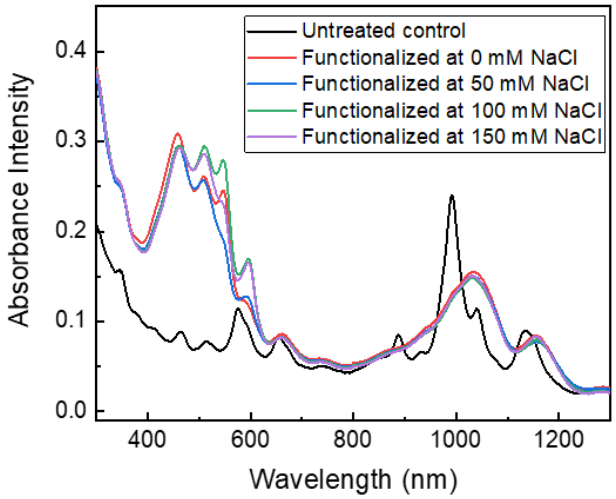

Fig. S3. Absorbance of functionalized SWCNTs at various salt concentrations. The reactive sequence used is GGGCGC.

Discussion on Fig. S3: Ionic strength could tune the stiffness of ssDNA and may exert influence on lattice modification of different (*n*, *m*) species. To directly test the effect of ionic strength, we conducted reactions at 0, 50, 100 and 150 mM NaCl (higher concentrations cause colloidal instability) to functionalize a (*n*, *m*) mixture (SG65i), which contains near-armchair (6,5), near-zigzag (9,1), and other chiralities in between. We reasoned that any (*n*, *m*)-dependent change in functionalization will cause spectral peak position and linewidth change. We therefore monitored reaction product by absorbance spectroscopy. **Fig. S3** shows the absorbance data, which indicates that RB consumption (absorption in the 400-600 nm) varies a little bit, but the absorption bands of functionalized SWCNTs in the 800 to 1300 nm region are insensitive to changes in salt concentration, implying that the profile of functionalized tubes remains constant.

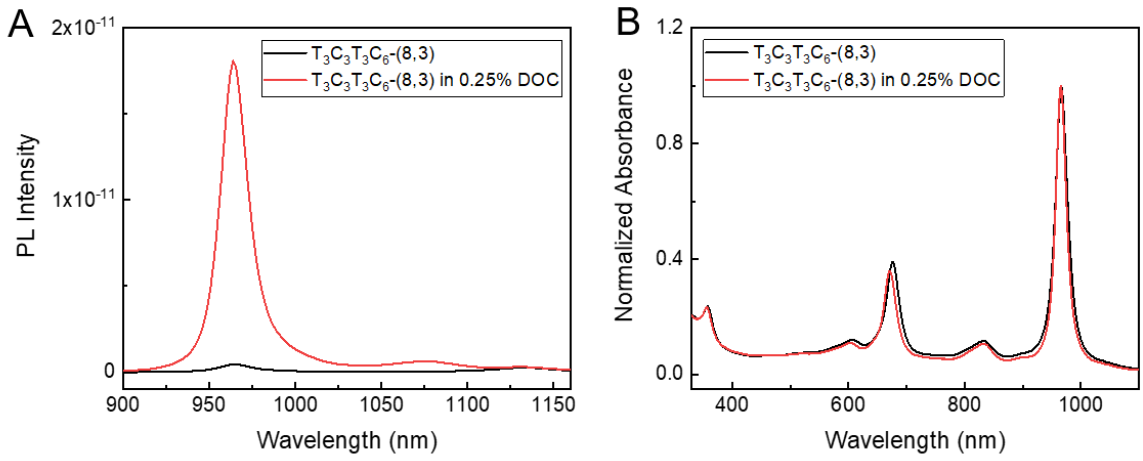

Fig. S4. (A) PL and (B) absorbance spectra of $T_3C_3T_3C_6$-(8,3) before and after adding 0.25% (w/w) DOC.

Discussion on Fig. S4: While DOC replacement of DNA is well-documented in the literature (*6*), to further illustrate the existence of DOC-coated SWCNTs in our case, we conducted experiments to monitor PL and absorbance change upon addition of DOC to $T_3C_3T_3C_6$-wrapped

(8,3). As shown in **Fig. S4**, addition of DOC causes a 40-fold PL increase and blue-shifted E_{11} and E_{22} absorbance peaks, indicating formation of new species.

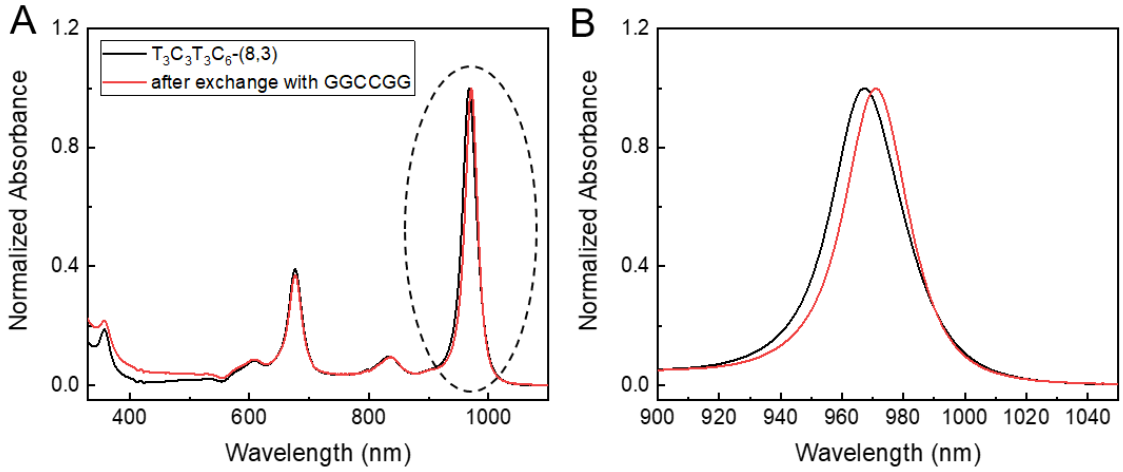

Fig. S5. (A) Absorbance spectra of $T_3C_3T_3C_6$-(8,3) before and after exchange with GGCCGG. (B) Zoomed-in view of E_{11} peak in panel A.

Discussion on Fig. S5: In the one-pot reaction, DNA/DNA exchange is mediated by DOC washing of the original wrapping sequence, and ~ 50-times higher concentration of G-containing sequence over original wrapping DNA ($T_3C_3T_3C_6$) for the rewrapping process. We designed an experiment to demonstrate that DNA/DNA exchange indeed takes place under this condition. A clear red-shifted E_{11} peak can be observed after $T_3C_3T_3C_6$-(8,3) was replaced by GGCCGG (**Fig. S5**).

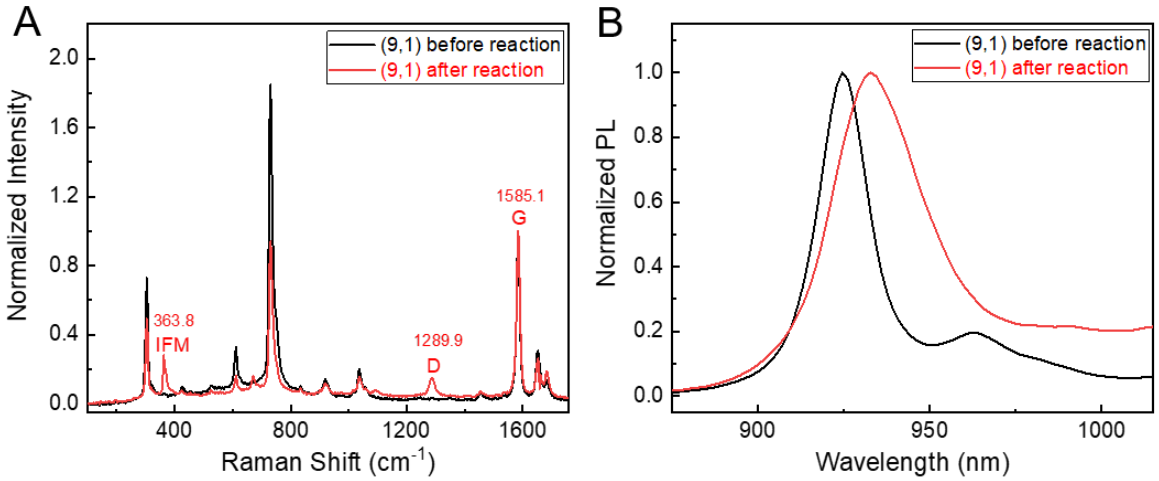

Fig. S6. Spectral characterization of (9,1) before and after reaction. (A) Raman spectra (normalized at the G peak); (B) Normalized PL spectra. The reactive G-containing sequence is $(GCGCCC)_6$. Spectra in A and B are measured with 671 nm excitation.

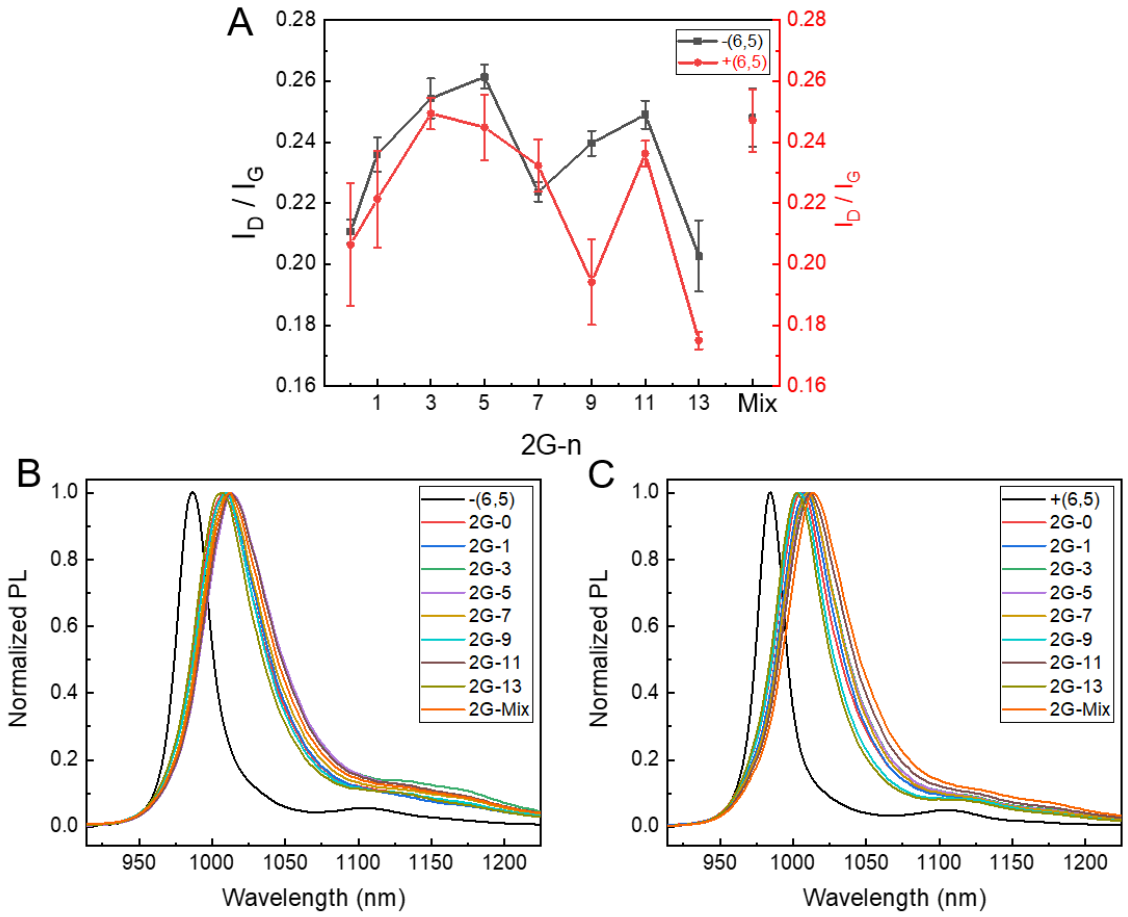

Fig. S7. Raman and PL spectroscopy characterization of ±(6,5) functionalized with sequences of 2G-n. (A) D peak intensity of ±(6,5) as a function of sequence pattern; (B) and (C) PL spectra of –(6,5) and +(6,5) as a function of sequence pattern. Spectra are measured with 532 nm excitation.

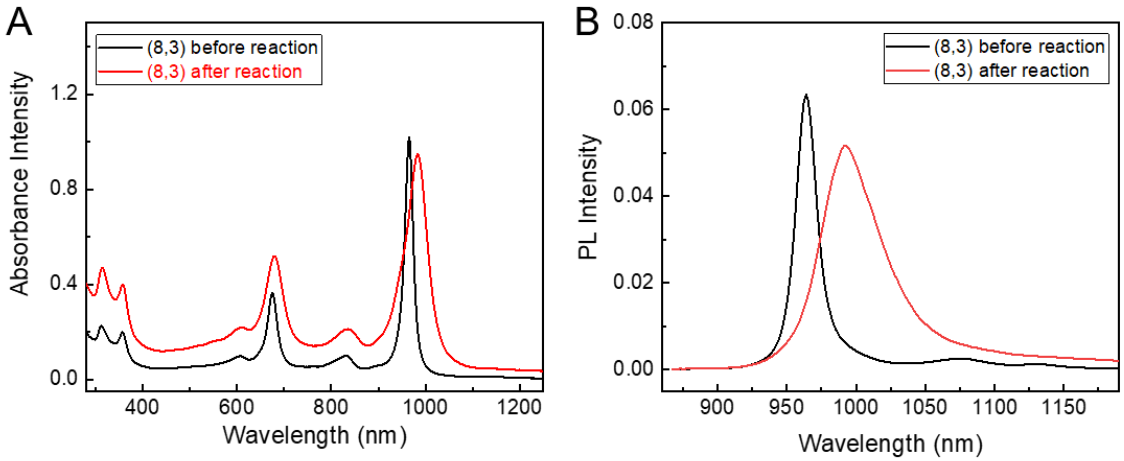

Fig. S8. Original data of (A) absorbance, (B) PL for **Fig. 1**. Spectra in B are measured with 671

nm excitation.

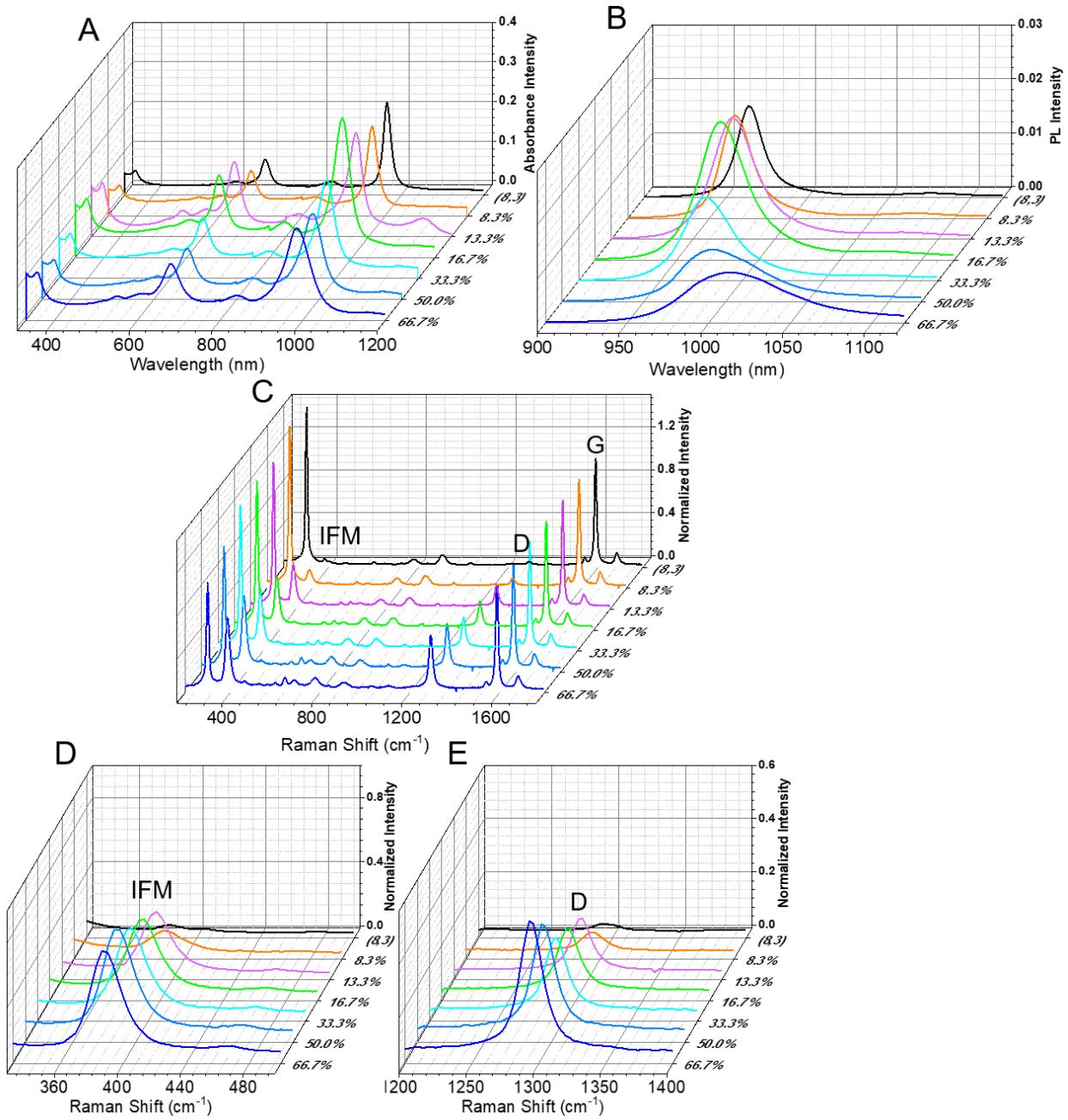

Fig. S9. Original data of (A) absorbance, (B) PL, (C, D, E) Raman spectra for **Fig. 2**. Spectra in B-D are measured with 671 nm excitation.

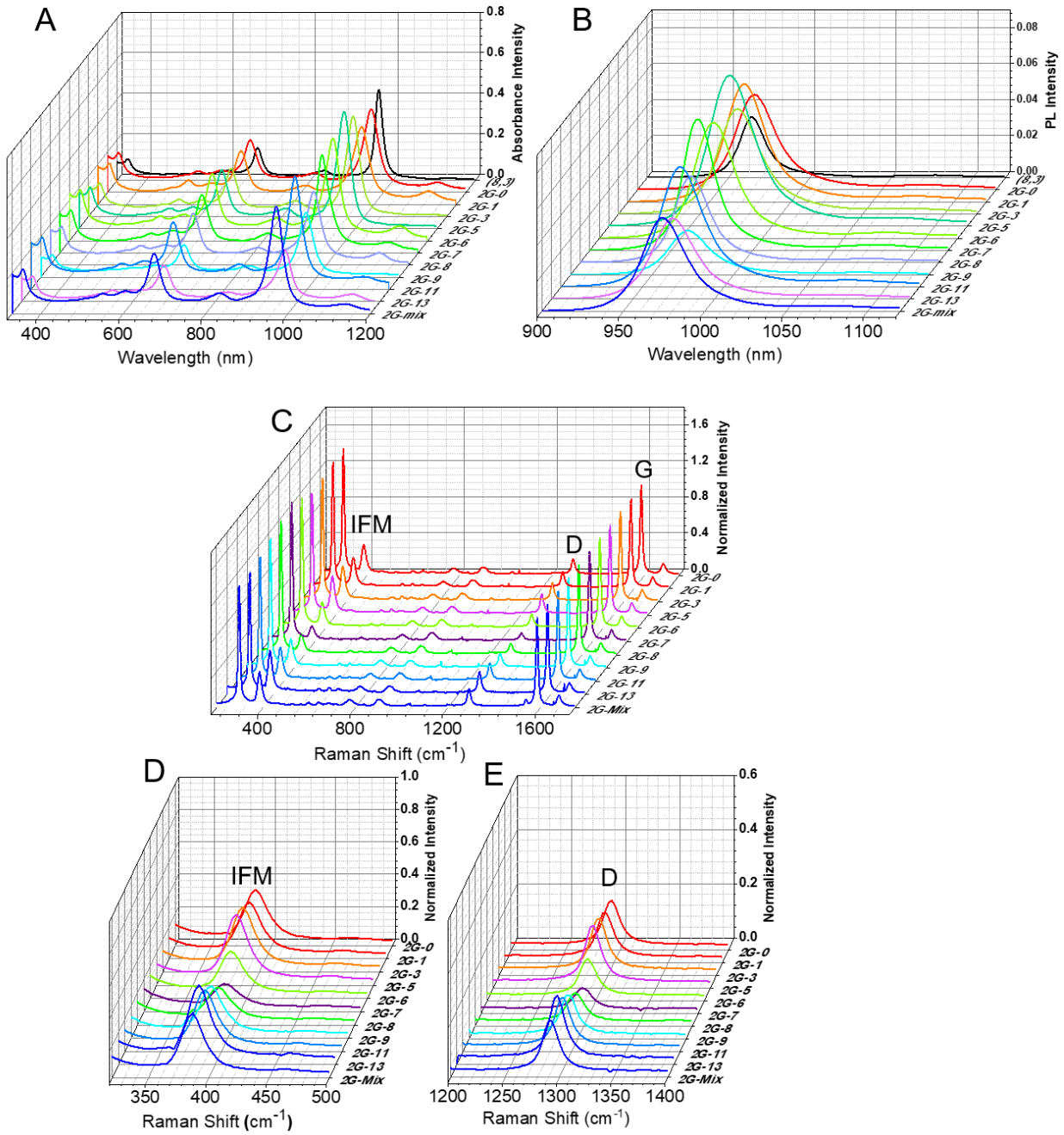

Fig. S10. Original data of (A) absorbance, (B) PL, (C, D, E) Raman spectra for **Fig. 3**. Spectra in B-D are measured with 671 nm excitation.

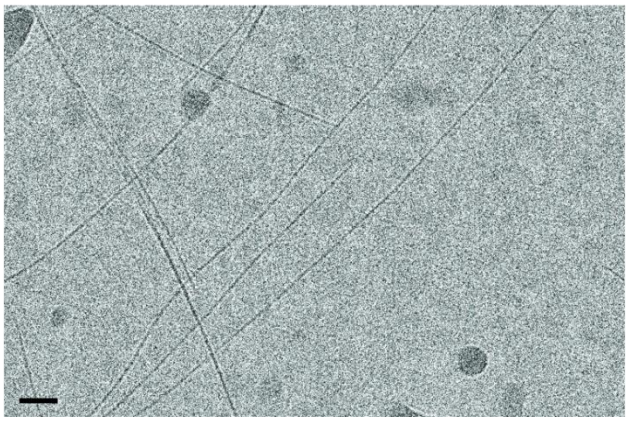

Fig. S11. A representative cryo-EM micrograph of 2G-7-functionalized (8,3). Scale bar 20 nm.

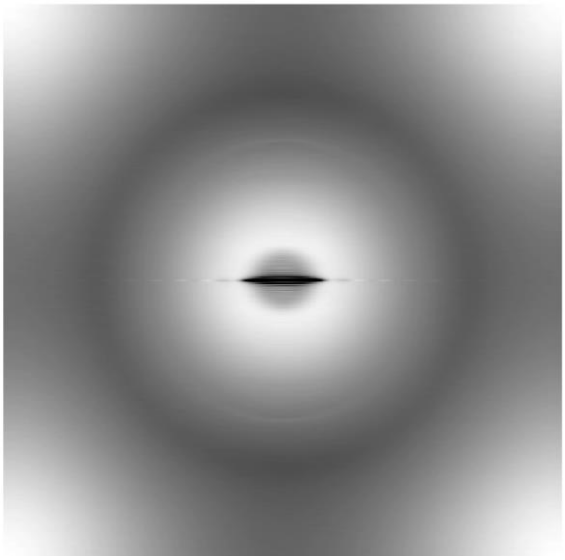

Fig. S12. Cryo-EM data of the control unfunctionalized 2G-7-(8,3). Averaged power spectrum of approximately 200000 particles, showing no periodicities.

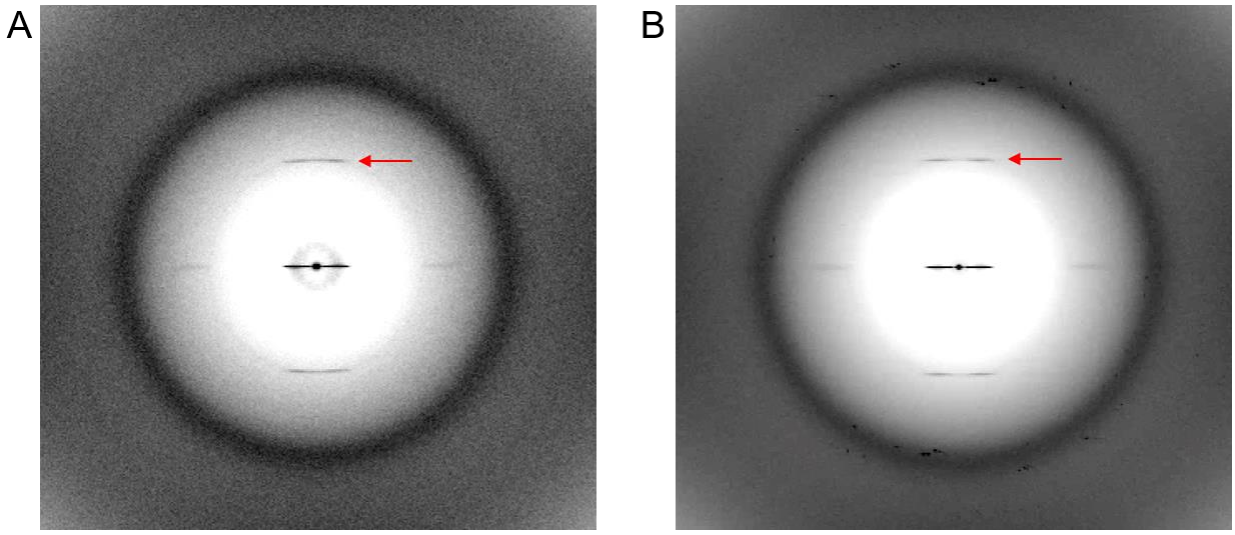

Fig. S13. (A) Averaged power spectrum of 2G-5-functionalized-(8,3); (B) Averaged power spectrum of 2G-6-functionlized-(8,3). Red arrow points to a layer line with a spacing of 1/(6.5 Å) from the equator.

Discussion on Fig. S13: The cryo-EM results in **Fig. S13** reinforce the reaction mechanism that G reacts with C-C bonds of maximum curvature to pin the DNA sequence on an armchair line. While cryo-EM detects the order of the overall wrapping structure, it does not have enough resolution to determine the location of Gs. Spectroscopy, on the other hand, is more specific to the order of covalent functionalization sites. It shows that 2G-7 has the smallest disorder (**Fig. 3**), which we interpret as due to all the G functionalized sites for this sequence being equally spaced along the armchair line.

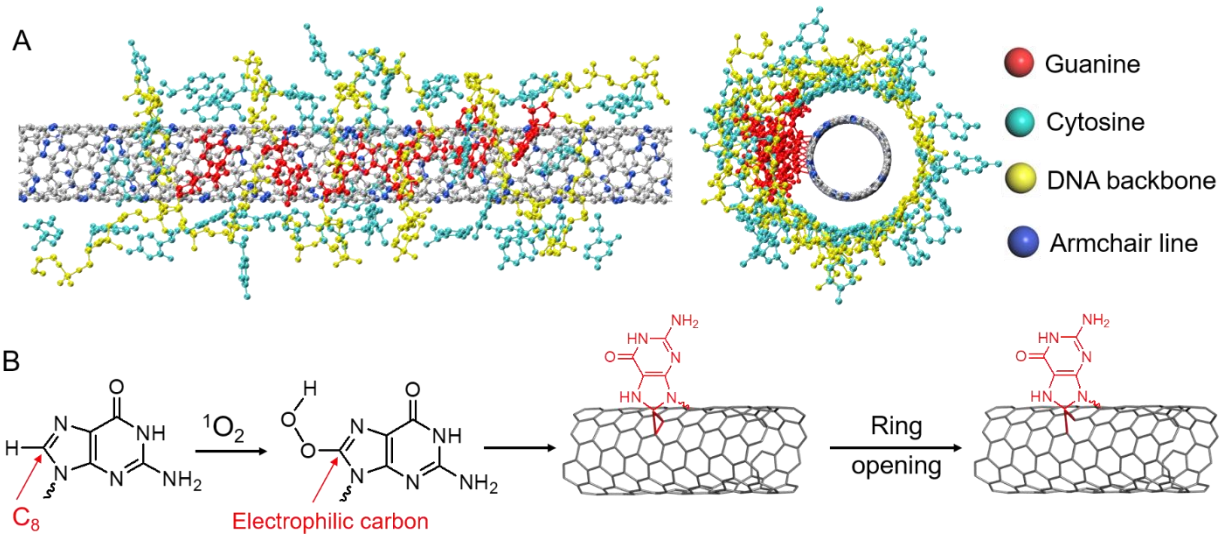

Fig. S14. (A) Modeling of 2G-7-functionalized (8,3), (B) A proposed reaction mechanism.

References

27. G. Ao, C. Y. Khripin, M. Zheng, DNA-Controlled Partition of Carbon Nanotubes in Polymer Aqueous Two-Phase Systems. *Journal of the American Chemical Society* **136**, 10383-10392 (2014).
28. G. Ao, J. K. Streit, J. A. Fagan, M. Zheng, Differentiating Left- and Right-Handed Carbon Nanotubes by DNA. *Journal of the American Chemical Society* **138**, 16677-16685 (2016).
29. Z. A. De los Santos, Z. Lin, M. Zheng, Optical Detection of Stereoselective Interactions with DNA-Wrapped Single-Wall Carbon Nanotubes. *Journal of the American Chemical Society* **143**, 20628-20632 (2021).
30. M. Lyu, B. Meany, J. Yang, Y. Li, M. Zheng, Toward Complete Resolution of DNA/Carbon Nanotube Hybrids by Aqueous Two-Phase Systems. *Journal of the American Chemical Society* **141**, 20177-20186 (2019).